

ORIGINAL ARTICLE

Open Access



Capacitive Imaging Technique for the Inspection of Composite Sucker Rod

Kefan Wang, Xiaokang Yin^{*} , Chen Li, Wei Li and Guoming Chen

Abstract

Composite sucker rod has been extensively used due to its high strength, light weight and corrosion resistive nature. However, such composite sucker rod is difficult for conventional non-destructive evaluation (NDE) techniques to inspect because of its complex material and/or structure. It is thus useful to embark research on developing novel NDE technique to comply the inspection requirement. This work demonstrates the feasibility of using the capacitive imaging (CI) technique for the inspection of composite sucker rod. Finite element (FE) models were constructed in COMSOL to simulate the detection of defects in the glass-fiber layer and on the carbon core surface. An FE Model based inversion method is proposed to obtain the profile of the carbon core. Preliminary CI experimental results are then presented, including the detection of surface wearing defect in the glass-fiber layer, and obtaining the profile of the carbon core. A set of accelerated aging experiments were also carried out and the results indicate that the CI technique is potentially useful in evaluating the ageing status of such composite sucker rod. The CI technique described in this work shows great potential to target some challenging tasks faced in the non-destructive evaluation of composite sucker rod, including quality control, defect detection and ageing assessment.

Keywords: Non-destructive evaluation, Capacitive imaging, Composite inspection

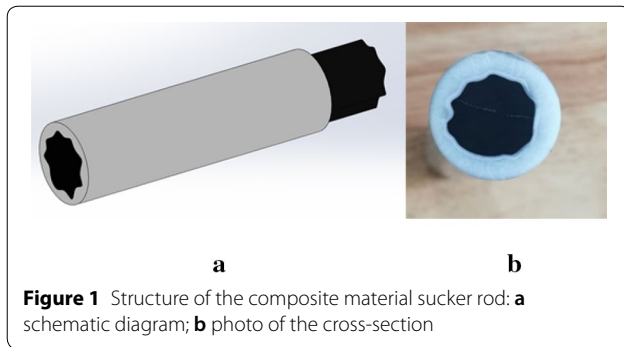
1 Introduction

Sucker rods are the long and thin rods attached to a pumping unit at the surface and extended down into an oil production well. They are connected to a pump at the bottom of the well, which is often more than 2000 m below the surface. Conventional sucker rods are usually made of steel. Such steel rods are limited in fatigue strength (particularly in tension), and can limit how deep of a well can be pumped, simply due to the weight of the rods. In recent years, composite sucker rods have been manufactured and extensively used in the oil and gas industry for a variety of reasons, including high strength, corrosion resistive and light weight. Such sucker rods are particularly suitable for Shengli Oilfield (Dongying, China), where the oil production wells are normally very deep (over 2000 m) and the underground environment is usually harsh (high temperature and highly corrosive). To guarantee safe operation, the integrity of the sucker

rod has to be ensured. This requires thorough evaluation of the sucker rod during its manufacturing and in-service stages. In this work, the capacitive imaging (CI) technique is adopted and its feasibility of defect detection and quality evaluation of composite sucker rod is demonstrated.

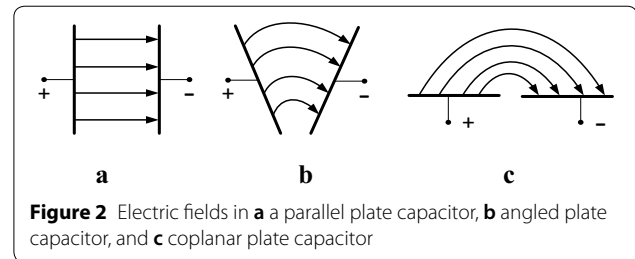
The composite sucker rod studied in this work is a carbon fiber pultruded multi-layer structure, which is shown in Figure 1. It's a hybrid fiber-reinforced polymers (FRPs) structure possesses both advantages of carbon fiber reinforced polymer (CFRP) and glass fiber reinforced polymer (GFRP) [1–4]. The carbon fiber core is a reinforcement in the center with its surface covered by a layer of glass fiber mixed with resin. The carbon core has an irregular profile to increase friction between layers to further increase the overall strength. Due to the complicated production process, there might be geometric imperfections (i.e., eccentricity of the carbon core). In addition, during its service life in the harsh environment, many type of defects, such as wearing, cracks and ageing, could happen to the sucker rod. The above mentioned manufacturing and in service defects will greatly affect the performance of the

*Correspondence: Xiaokang.yin@upc.edu.cn
Centre for Offshore Engineering and Safety Technology, China University of Petroleum (East China), Qingdao 266580, China



sucker rod and can potentially lead to sucker rod failure. NDE techniques are thus required to spot such manufacture and service induced defects. There are many commercially available NDE techniques to detect defects in multi-layered composite material and structures, include ultrasound, X ray, infrared thermal imaging, and etc. Ultrasonic methods can detect the internal defects with composite materials [5–7]. X ray method can be used to detect voids, porosity, inclusions, and fiber breakage in composites [8]. Infrared thermal imaging can be used to detect deboning, delamination, cracks and inclusions in composites [9]. Microwave methods can be used to characterize various types of defects in composites [10]. The eddy current method can realize the detection of defects in conductive composite materials, such as CFRP, conductive plastics composite, and conductive rubber composite [11–13]. Pulsed eddy current technique was also used to detection impact damage in CFRP [14–16]. Other attempts using conventional NDE methods on the inspection of composite material, include the liquid permeation method, ultrasonic guided wave, thermography and acoustic emission method [17–20], are also reported in literature. Although the above mentioned techniques can cover almost all types of defects in composite materials, they are almost inapplicable for the composite sucker rod due to their inherent technical drawbacks. For example, the ultrasonic approach is difficult to implement in this case because the sucker rod is too thin (19 mm or 22 mm in diameter) for the transducer to have a reasonably high degree of coupling. The eddy current approach would not work on the outer non-conducting glass fiber layer. The X ray technique can easily be operated, but it has health/safety and cost issue.

The CI technique, which uses capacitive coupling between electrodes to inspect specimen, is adopted to target the challenges encountered in the composite sucker rod inspection. The principle of the CI technique is based on the fringing effect of electric field. Compared to some of the traditional NDE techniques, the CI technique has some unique features, such as it



is a non-contact technique, it only requires single side access to the specimen, and can work on a wide range of material types [21–24]. Therefore, the CI technique is widely used in the non-destructive testing field, such as humidity monitoring, ageing degree testing and compact damaging detection [25–30]. This paper describes the theory of this technique, the FE models and some experimental results to investigate the usefulness of the CI technique for the inspection and imaging of the composite sucker rod.

2 CI Technique and Probe Design

2.1 Principle of the CI Technique

The general principle of CI technique is shown in Figure 2. A capacitive probe is changed from being a parallel plate capacitor to a coplanar structure. When the capacitor is a parallel plate capacitor, with a DC energization a uniform electric field will be established between the parallel electrodes, as shown in Figure 2(a). If the parallel electrodes are opened at an angle as shown in Figure 2(b), the uniform electric field changes into a fringing field. Finally, if the parallel electrodes are further opened to be coplanar, the fringing electric field will become the main effect as shown in Figure 2(c). Exciting the driving electrode with a DC voltage will produce a fringing electric field which can induce charges on the sensing electrode and the amount will vary depending on the properties of material under test. The capacitive probe can then get the defects information by measuring the charges from the sensing electrode.

When used on the composite sucker rod, the probing electric field will penetrate through the air gap between the capacitive probe and the glass fiber layer of the rod, and form a certain field distribution in the glass fiber layer. Any anomaly within this layer will change the field distribution and ultimately change the capacitance. The electric field will then terminate on the conducting carbon core and form an equal-potential surface. The distance between the probe surface and carbon core surface (defined as lift-off) will also

change the capacitance. Therefore, the CI technique is considered useful to detect the defects in the glass fiber layer and characterize the surface of the carbon core, as shown in Figure 3.

2.2 CI Probe Design

To meet specific inspection requirements, the CI probe has to be designed and optimized. This can be achieved by analyzing the measurement sensitivity distribution. In this section, the measurement sensitivity distribution of capacitive probe is used as an indicative tool in the process of design. The measurement sensitivity distribution in the sensing area under a CI probe can effectively describe each region’s contribution to the signal change of the sensor and has been described in detail in our previous work [21]. Comparing sensitivity distributions of capacitive probes with different geometries, parameters that measure their imaging performance, such as penetration depth, signal strength and imaging resolution, can be inferred. The sensitivity distribution $s(x, y, z)$ in the sensing area of a capacitive probe can be described as:

$$s(x, y, z) = -\vec{E}_D \cdot \vec{E}_S, \tag{1}$$

where the \vec{E}_D and \vec{E}_S are the electric fields in the location of regions when the driving electrode and sensing electrode were stimulated by a unit voltage respectively. Such electric fields from reciprocal energization can be easily obtained in Finite Element models as described in detail in previous work [21]. Coplanar capacitive probe with two triangular electrodes is selected in this case, as the triangular electrode can balance the trade-offs in the probe design. The triangular probe can be specified by the overall width (W), the overall length (L), the base (b) and height (h) of each triangle and the separation distance (s) between the parallel edges of the two triangles as shown in Figure 4.

Three probes with specifications indicated in Table 1, were studied to identify suitable parameter combinations. The sensitivity distributions for the CI probes are show in Figure 5. Note that the sensitivity distribution a 3D, for a clearer illustration, only one cross-section

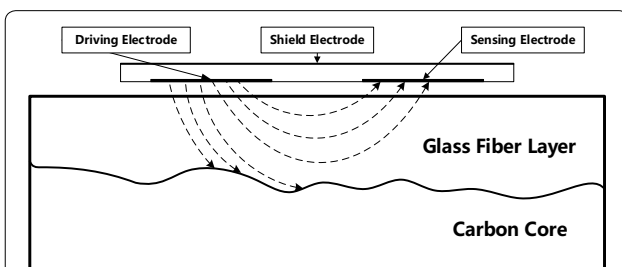


Figure 3 General principle of the CI technique used in the inspection of composite sucker rod

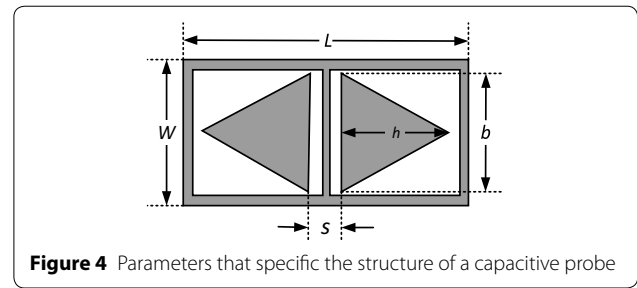


Figure 4 Parameters that specific the structure of a capacitive probe

along the long axis of symmetry of the CI probe is plotted. The color maps were set in the same range, so direct comparison can be made more accurately. As shown in Figure 5, the high sensitivity area (referred to as volume of interrogation) is bigger with the sensor size increases.

Bigger volume of interrogation means bigger inspection extent in a single measurement position, so from the sensitivity distribution map one can briefly infer the penetration depth and signal strength of a given CI probe. It can be seen from Figure 5 that Probe 1 can get about 4 mm penetration depth, Probe 2 is with an approximate 6 mm penetration depth and Probe 3 is with a 9 mm penetration depth. Generally, a bigger penetration depth is favorable in the CI measurement, but this is trade-off against imaging resolution. The diameter of the composite sucker rod studied in this work is 22 mm, and the thickness of the outer glass fiber layer is between 2 mm to 5 mm. A suitable CI probe should have a big enough penetration depth to cover the whole range of insulation layer and to have a relatively small volume of interrogation to have a reasonable imaging resolution. Therefore, Probe 2 (with a 6 mm penetration depth) was chosen for the later simulations and experiments.

For better measurement results, a slight modification was done to the coplanar CI probe. A flexible PCB was used to replace the conventional rigid FR4 PCB and a curved substrate was manufactured using 3D printing to fit the surface of the sucker rod specimen, as shown in Figure 6.

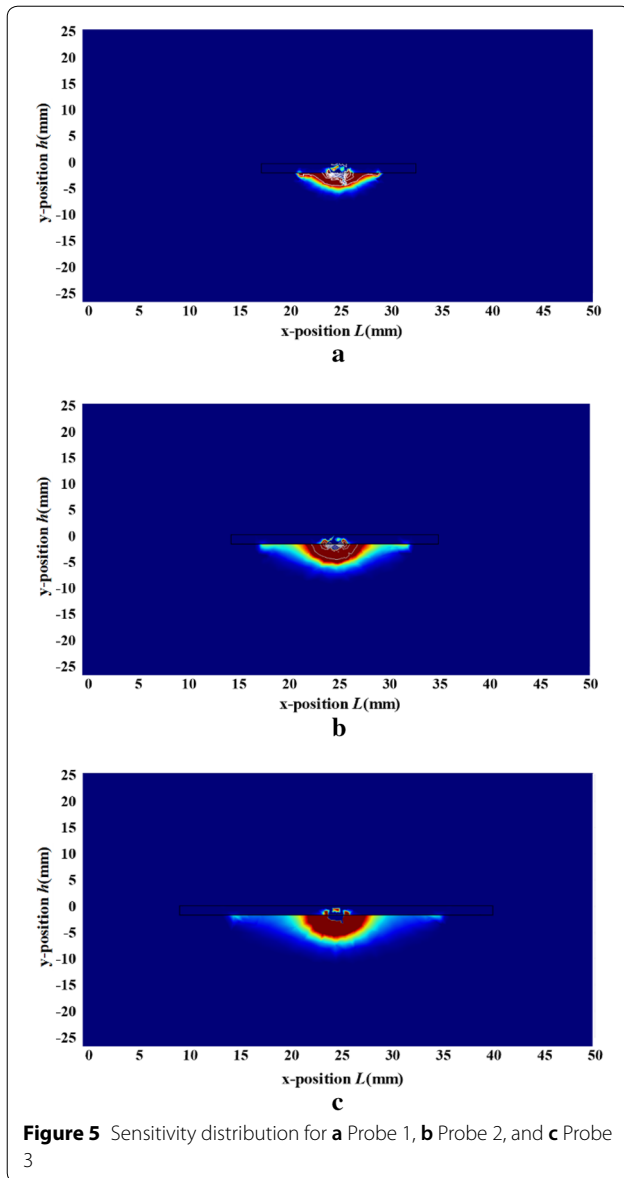
3 Finite Element (FE) Analysis

3.1 Model Setup

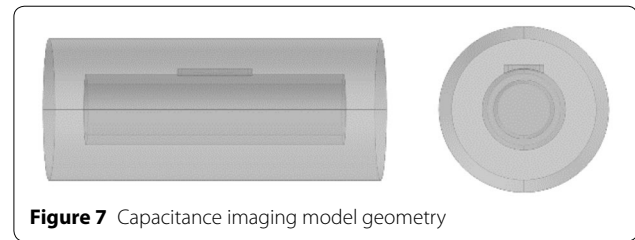
Finite element simulations were carried out in COMSOL Multiphysics software to confirm the feasibility

Table 1 Parameters for CI probes of different sizes

Probe	L (mm)	W (mm)	h (mm)	b (mm)	s (mm)
Probe 1	15	15	3	3	2
Probe 2	20	10	6	6	2
Probe 3	25	25	9	9	2



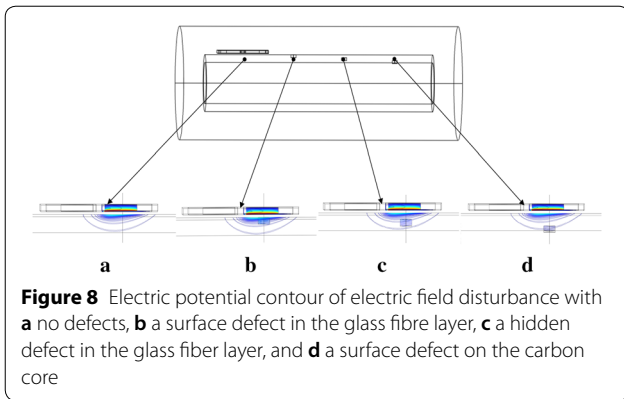
of the CI technique. The 3D model geometry is shown in Figure 7. The outer cylinder is the computational domain which is filled with air ($\epsilon = 1$) in the simulation.



The specifications of the capacitive probe are the same with the ones used in the experiments (shown in Figure 6). The simulated sucker rod comprises three layer including carbon fiber core (12 mm in diameter), glass fiber outer layer (4 mm thick) and a thin (1 mm) resin layer in between. The computational domain is $400\pi \times 90 \text{ mm}^3$ with 72535 elements after meshing. The diameter of the simulated sucker rod is 22 mm which is the same as the rods tested in the experiments as will be presented in Section 4. The material properties of three layers are set as follows: carbon fiber (fiber direction: axial, grounded conductor), glass fiber (fiber direction: circumferential direction, $\epsilon = 4.7$), and epoxy resin ($\epsilon = 3.5$). The driving electrode is energized by 1 V DC voltage and the sensing electrode is set to be “floating”. The back plane of the CI probe is set to be grounded as a shielding. Other boundaries in the model are set to be “continuity”. The capacitances are calculated between the driving and sensing electrode.

3.2 Electric Field Disturbance Due to Defects

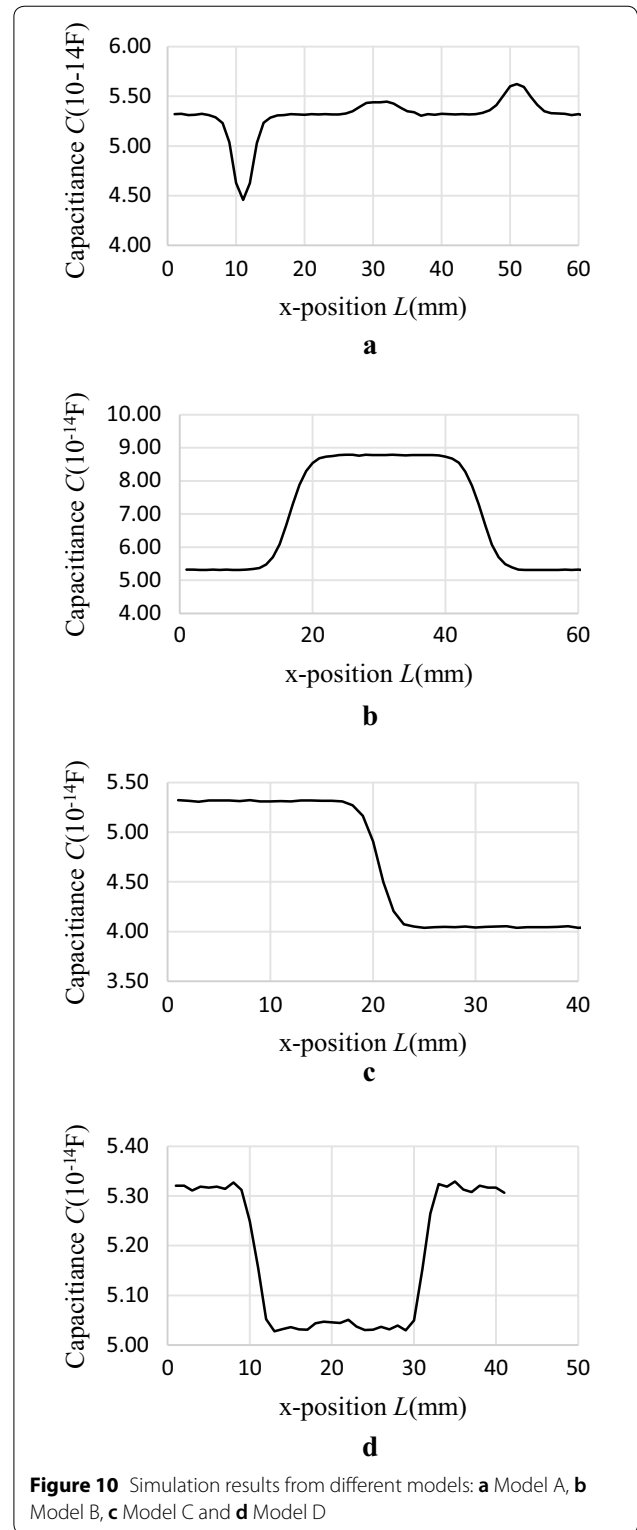
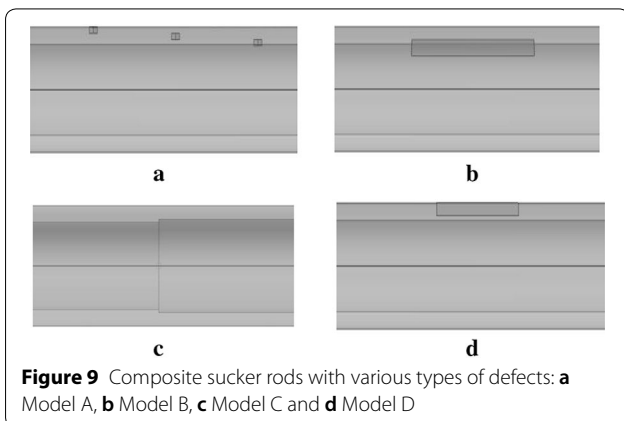
It has been demonstrated in previous work that defects at different positions in the sensing area can have different influence on the experimental results [25]. It is thus useful to study how the defects in various positions of the composite sucker rod disturb the probing electric field. Three cylinder voids (1 mm height and 1 mm radius) to simulate three distinct defects in the composite sucker rod are introduced in the 3D FE model, namely surface defect in glass fiber layer, hidden defect in glass fiber layer and surface defect on carbon core, as shown in Figure 8. The computational domain is $400\pi \times 110 \text{ mm}^3$ with 99831 elements after meshing. A Simulated CI scan was performed in the FE model with the CI probe moved along a line that passing through the three defects. Electric potential plot is chosen to illustrate the field disturbance due to defects. Three instants in the line scan when the CI probe is right on top of the three defects, together with one instant with the probe being on top of a sound part, are plotted as shown in Figure 8. It can be seen from Figure 8 that the electric potential contours are altered at the defected areas in all the three cases, indicating the promise of defect detection in the composite sucker rod using the proposed method.



3.3 Simulated Defect Detection in FE Models

The feasibility of defect detection using the CI technique is further demonstrated with simulated CI scans on composite sucker rod with various types of defects. Four models with commonly seen defects are built in COMSOL, as shown in Figure 9. The first model (Model A) is with three voids at different depths in the glass fiber layer, as shown in Figure 9(a). The voids are cylinders with 0.5 mm bottom radius and 1 mm height. The second model (Model B) is with a layered defect lies on the interface between the glass fiber layer and the carbon core, as shown in Figure 9(b). The dimension of the layered defect 2 mm (width) by 0.2 mm (depth) by 20 mm (length). The third model (Model C) is with a carbon core of stepped diameters (0.5 mm difference), as shown in Figure 9(c). The fourth model (Model D) is with a surface breaking crack in the glass fiber layer, as shown in Figure 9(d). The dimension of the crack is 0.2 mm (width) by 2 mm (depth) by 20 mm (length).

Simulated scans were performed with a CI probe scanned along the axial direction in the four models and the results are shown in Figure 10. All the three defects in Model A produced clear indications in the line scan



results, as shown in Figure 10(a). The three defects at different buried depth produced different capacitance variation trends, one defect appeared as a depression and

the other two appeared as bulges. In this simulated scan, same type of defects produced different indications. This is due to the distribution of negative measurement sensitivity values. If a defect is situated in a negative measurement sensitivity value zone, it will bring in opposite contributions to the measured capacitance [31]. The layered defect in Model B were detected as a clear bulge, as shown in Figure 10(b). The carbon core with stepped diameter in Model C is clearly shown as a step shaped curve, as shown in Figure 10(c). The surface crack in Model D is also successfully detected as a depression in the obtained capacitance plot, as shown in Figure 10(d). The results from the four models further demonstrated the feasibility of the CI technique to detect various types of defect in the composite sucker rod.

3.4 Simulated Carbon Core Profile Inversion in FE Models

The carbon core of the composite sucker rod usually has an irregular profile of its cross-section to enhance the strength. The fluctuant surface is not regarded as local defect in general. However, the complex pultrusion manufacturing process might bring in geometric defects, such as the eccentricity of the carbon core and shrunk/expanded carbon core cross-section area. Such geometric defects will significantly reduce the strength of the entire sucker rod. It is thus important to obtain the profile, as a quality control measure. As discussed in Section 2.1, CI probe is sensitive to uneven surface of the carbon core. If scanned around the circumference of the sucker rod, the CI output will reflect the profile of the carbon core. However, to obtain the actual profile of the core, post processing of the obtained data is required. An inversion method is proposed and implemented in an FE model. A composite sucker rod with a pentagon-like shaped carbon core was constructed in the FE model, and the carbon core cross-section is shown in Figure 11.

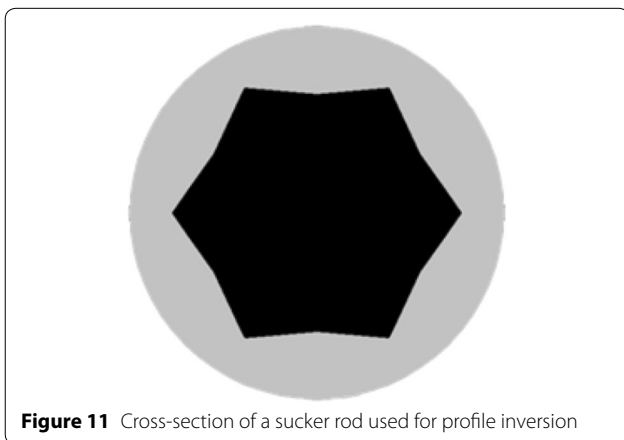


Figure 11 Cross-section of a sucker rod used for profile inversion

A simulated CI line scan along the circumference of the sucker rod was performed using the curved CI probe at a minimal lift-off. The calculated capacitance values at each scan point is plotted in the polar coordinate, as shown in Figure 12. It is obvious that Figure 12 is not the outer profile of the carbon core as the radius in the polar plot is measured (calculated) capacitance value, rather than the actual radius of the carbon core.

A relationship between measured (calculated) capacitance value and the radius of the core is thus required to map the polar plot of capacitance values to the profile of the carbon core. To find this relationship, a parametric FE model is built. In this model, the capacitance values of the CI probe with increased lift-offs (equivalent to the thicknesses of the glass fiber layer) at a 0.2 mm interval are obtained. A fitting curve of the calculated capacitance values (C) against lift-offs (d) is shown in Figure 13 and the fitting formula is:

$$C = x_1 d^5 + x_2 d^4 + x_3 d^3 + x_4 d^2 + x_5 d + x_6, \quad (2)$$

where $x_1 = -7.468^{-19}$, $x_2 = 2.226^{-17}$, $x_3 = -2.316^{-16}$, $x_4 = 8.141^{-16}d$, $x_5 = 1.762^{-15}d$, $x_6 = -7.226^{-15}$.

A clear non-linearity can be observed in Figure 13.

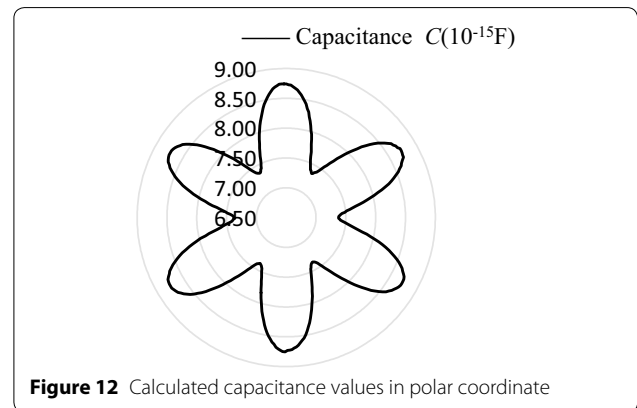


Figure 12 Calculated capacitance values in polar coordinate

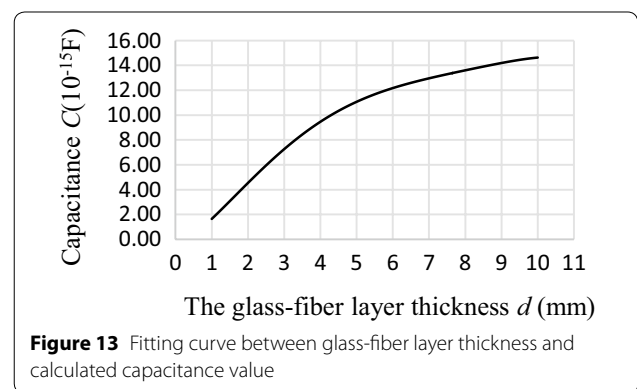


Figure 13 Fitting curve between glass-fiber layer thickness and calculated capacitance value

The fitting formula is then used to calculate the actual lift-offs d (the thickness of the glass fiber layer), and the real radius of the carbon core at each scanning step can finally be obtained by subtracting the d value from the radius of the sucker rod (11 mm in this case). The final inversion result is shown Figure 14. Comparing Figure 14 and Figure 11, the profile of the carbon core is roughly reflected from the CI data after the proposed inversion method. It should be noted that, the obtained plot is not as sharp as the actual profile, because the CI probe works in a volume averaging manner thus has a blurring effect. The blurring effect is more significant in the cases when the probe size is bigger compared to the targeted feature.

4 CI Experiments on the Composite Sucker Rods

4.1 Experimental Setup

The CI signal generating and processing system includes a signal generator (Tektronix AFG1022 Arbitrary Function Generator), a charge amplifier (Conditioning Amplifier type LC0601), a lock-in amplifier (Signal Recovery Model 7230 DSP Lock-in amplifier), an oscilloscope (Tektronix TDS 1072B Digital Oscilloscope), and an NI PXI system. The motion control system includes an X - Y - Z three-axis scanning stage and an R - θ rotary stage for the motion control in the scanning experiments. The schematic diagram and the photo of the CI instrument are shown in Figure 15.

With the above mentioned instrument, an AC capacitance measurement method is used to achieve a better signal to noise ratio. The driving electrode of the CI probe is excited by the signal generator with an AC voltage (10 V pk-pk @ 10 kHz). At 10 kHz, the quasi-static approximation is appropriate and the probing field can be regarded as a static electric field. Therefore, the statements and analysis made in Section 2.1 are valid. The charge signal induced on the sensing electrode is taken by the charge amplifier and converted to a voltage. The voltage signal is then fed into the dual channel lock in amplifier, and the DC output from the lock-in amplifier is recorded by the NI PXI system. The motion control

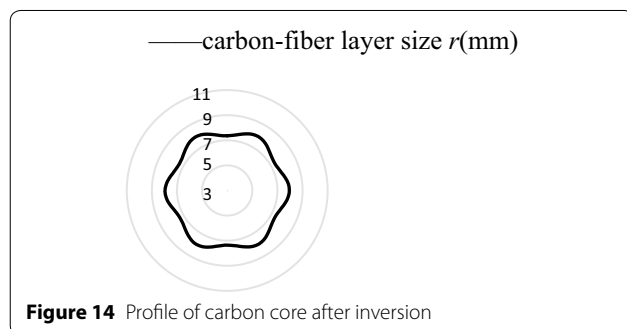


Figure 14 Profile of carbon core after inversion

system can manipulate the CI probe to perform an actual scan. Software developed in LabVIEW is installed in the NI PXI system for data acquisition and motion control.

4.2 Detect Wearing Defect on the Sucker Rod Surface

CI experiment was performed on a composite sucker rod specimen with a surface wearing defect. The wearing defect was made in the lab and is very shallow (less than 0.1 mm), as shown in Figure 16. In practice, such slight wearing defect may not be easily seen as its color may be very close to its surrounding area. A 60 mm by 10 mm CI scan was performed in the boxed area indicated in Figure 16 and the capacitive image is shown in Figure 17. It can be seen from Figure 17 that, the wearing defect is clearly seen in the capacitive image. Note that there are

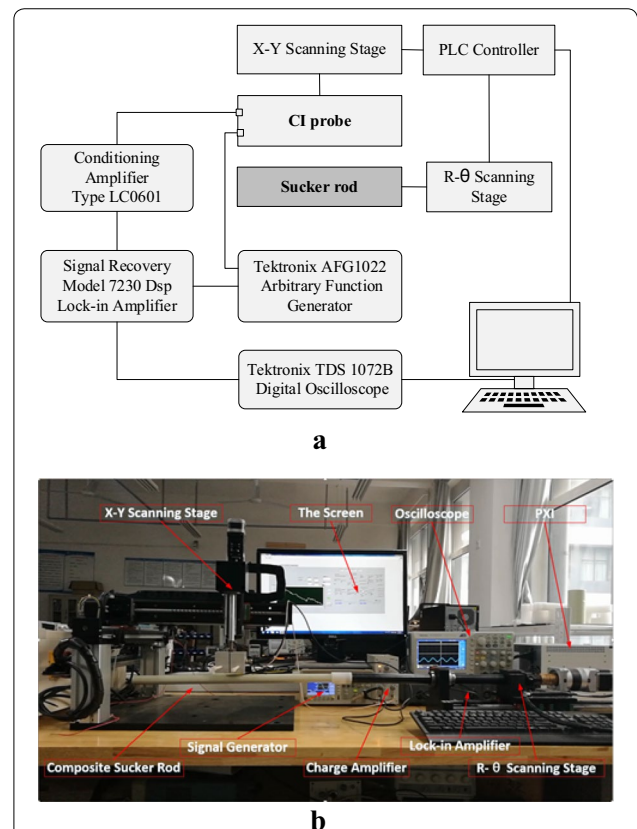


Figure 15 Capacitance imaging instrument: a block diagram, and b photo of the instrument

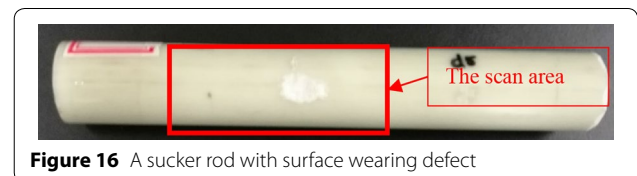


Figure 16 A sucker rod with surface wearing defect

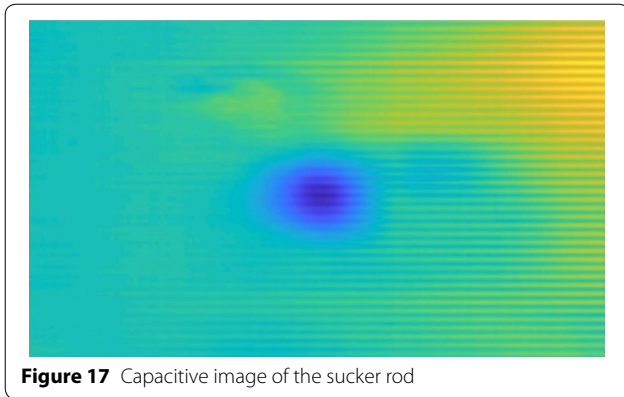


Figure 17 Capacitive image of the sucker rod

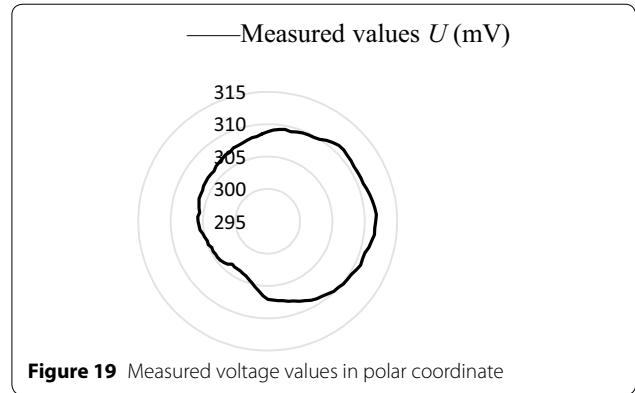


Figure 19 Measured voltage values in polar coordinate



Figure 18 Cross-section of a sucker rod

intensity variations in the background (defect free) area due to the uneven surface of the carbon core.

4.3 Carbon Core Profile Inversion in Experiment

A CI scan was done in an attempt to obtain the carbon core profile and verify the inversion method proposed in Section 3.4. The cross-section of the sucker rod is shown in Figure 18.

The CI probe was scanned around the circumference of the sucker rod. Firstly, as in Section 3.4, the measured value is directly plotted in the polar coordinate, as shown in Figure 19.

To get the profile of the carbon core, a relationship between the measured value and the radius at the scan position is required. However the fitted curve and the fitting formula obtained in Section 3.4 cannot be used directly, because the output in the CI experiments is not a capacitance value but a voltage. An additional step, which is obtaining the relationship between the calculated capacitance in FE model and measured voltage output in experiment, is thus required to modify the fitted curve and the

Table 2 Experiment and simulation results for selected points

Thicknesses of glass-fiber layer d (mm)	CI readings U (mV)	Simulation results C (10^{-15} F)
2.5	303.6	5.96
3.5	307.05	8.47
4.1	308.5	9.65

fitting formula obtained in Section 3.4. The CI instrument is a linear measurement system with fixed overall gain and DC drift. Therefore, the relationship between the calculated capacitance in FE model and measured voltage output in experiment should be linear. Three CI readings taken at know lift-offs are used to find the linear relation between calculated capacitance in FE model and measured voltage output in experiment, the selected points are shown in Table 2. The three measurement points are with 2.5 mm, 3.5 mm and 4.1 mm glass fiber layer thickness. CI readings at these selected points were taken. Combining with the simulated results in Section 3.4, a relation between the measured voltages (U) and capacitance values (C) from simulation can be established. The fitted line is shown in Figure 20 and the corresponding fitting formula is:

$$U = 1.332^{15}C + 295.7, \tag{3}$$

where U is the voltage value recorded in experiments and C is the calculated capacitance in the FE model.

Finally, combing Eq. (2) and Eq. (3), a curve of the measured voltage (U) against lift-offs (d) can be obtained and is shown in Figure 21. The corresponding fitting formula is:

$$U_c = x_1d^5 + x_2d^4 + x_3d^3 + x_4d^2 + x_5d + x_6, \tag{4}$$

where $x_1 = -9.89^{-4}$, $x_2 = 2.949^{-2}$, $x_3 = -0.3069$, $x_4 = 1.079$, $x_5 = 2.334$, and $x_6 = 294.7$.

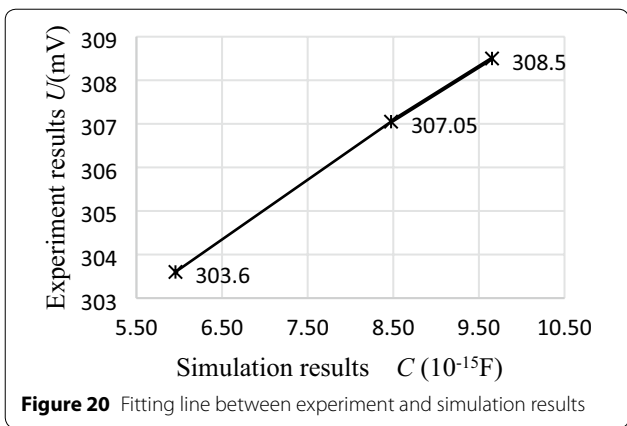


Figure 20 Fitting line between experiment and simulation results

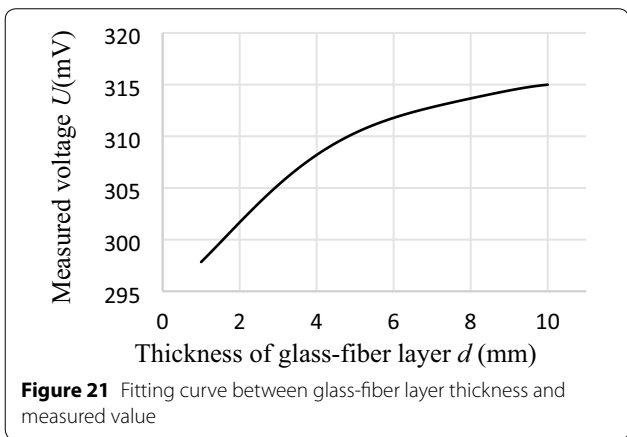


Figure 21 Fitting curve between glass-fiber layer thickness and measured value

The fitting formula (Eq. (4)) can then be used to calculate the actual lift-offs d (the thickness of the glass fiber layer), and real radius of the carbon core at each scanning step can finally be obtained by subtracting the d value from the radius of the sucker rod (11 mm in this case). The final inversion result is shown as white line in Figure 22. The actual cross-section of the sucker rod in also included for direct comparison. Although the obtained plot is not as sharp as the actual profile, the profile of the carbon core can be roughly reflected from the CI data after the proposed inversion method. The rapid change of the carbon core profile (e.g., the bottom-right part) is “ignored” by the CI probe, because the CI probe is less sensitive to features much smaller compared to its size.

4.4 Evaluation of Aged Composite Sucker Rod

One of the biggest issues of the composite sucker rod during its long-term service process is that the composite material will degrade. Because of lengthy direct exposure to high-temperature immersion in

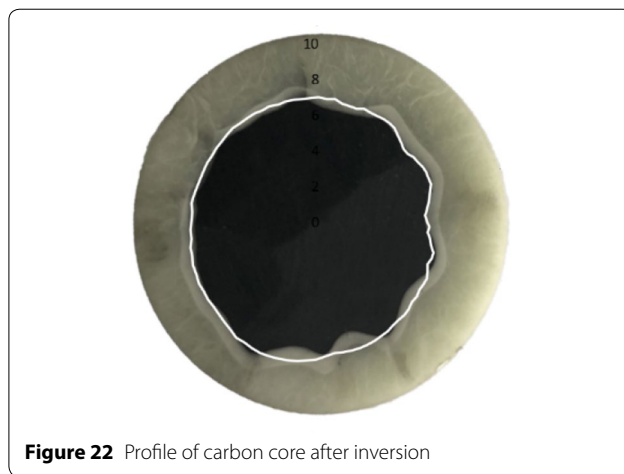


Figure 22 Profile of carbon core after inversion

water under hydraulic pressure, ageing is more likely to occur in such composite sucker rod. The glass fiber layer is prone to degrade owing to hydrolysis, plasticization, swelling of matrices and debonding of fiber/matrices when exposed to hydrothermal conditions [31]. Such degradation will greatly affect the in-service performance. Therefore, the long-term properties of the composite sucker rod need to be fully understood. Evaluation tools are needed to determine the ageing stages of composite sucker rod. In this section, CI technique is employed to evaluate composite sucker rod specimens after accelerated ageing.

A composite sucker rod specimen was selected to perform the ageing evaluation trials. Three measurement points were chosen on the sucker rod. Capacitive measurements were taken on the three points before ageing as references. The sucker rod was then placed in an ageing vessel for hydraulic pressure immersion. An ageing condition of 60 °C and 15 MPa hydraulic pressure was used. The selected ageing temperature and the hydraulic pressure were determined to reflect the practical service condition.

For the first stage, the ageing time was 7 d. After that, the specimen was taken out from the vessel, kept in a desiccator for a day, and capacitive measurements were taken on the three selected points. For the second stage, the ageing time is another 7 d. Again, the specimen was taken out from the vessel, kept in a desiccator for two day, and capacitive measurements were taken on the three selected points. The capacitance values at the selected point before and after the two stages’ ageing are listed in Table 3. It can be seen that the measurement voltages changed significantly before and after ageing. In addition, comparing the results after the two ageing stages, the measured voltages also changed. This

Table 3 Ageing experiment results

Measurement points	Measured value before ageing U (mV)	Measured value after 7 d of ageing U (mV)	Measured value after 14 d of ageing U (mV)
1	106.7	118.5	127.12
2	106.9	112.13	138.3
3	106.6	115.833	121.3

indicates the CI probe is sensitive to water absorption and/or material degradation caused by ageing.

5 Conclusions

Composite sucker rod is a difficult structure for conventional NDE technique to deal with, due to its shape and complex material contents. The CI approach described in this work aims to offer a possible route to overcome some of the limitations imposed by existing NDE techniques for the inspection of composite sucker rod. The technique is investigated in some depth to further evaluate its possible application to composite sucker rod.

- (1) The principle of the CI technique is briefly introduced. A triangular electrode probe with $b=6$ mm, $h=6$ mm and $s=2$ mm was found to be optimum in terms of the trade-offs in sensitivity (increased by a larger electrode size) and resolution for the inspection of sucker rod studied in this work. This choice was confirmed by a comprehensive measurement sensitivity distribution studies.
- (2) The FE models shows that the CI technique is promising in detecting defects in the outer glass fiber layer and on the conducting carbon core surface. A model based inversion method to obtain the profile of the carbon core is proposed.
- (3) It can be seen from the experimental results that the CI technique is sensitive to various types of defects in the composite sucker rod. Both surface wearing and uneven carbon core surface were successfully imaged. The profile inversion method is also verified on a sucker rod specimen.
- (4) Capacitive measurements on aged sucker rod specimen indicate that the CI technique is useful to evaluate the ageing status of the sucker rod.

It should be noted that the intention is to demonstrate the potential of capacitive techniques to detect artefacts within the composite sucker rod. Thus, the defects introduced in the samples, and the conditions under which they were tested (both in FE models and experiments), were designed to provide clear results

rather than exactly simulate in-service situations. Work including developing on-site measurement CI probe with multiple electrode pair combinations for industrial applications is currently being performed.

Acknowledgements

The authors would like to thank Mr. Feng Li, Mr. Anquan Wang and Mr. Jianfei Chen from Sinopec Shengli Oilfield Technology Inspection Centre for providing the specimens.

Authors' Contributions

XY, WL and GC were in charge of the whole trial; XY and KW wrote the manuscript; CL assisted with sampling and laboratory analyses. All authors read and approved the final manuscript.

Authors' Information

Kefan Wang, born in 1994, is currently a master candidate at *Center for Offshore Engineering and Safety Technology, China University of Petroleum*. He received his bachelor degree from *China University of Petroleum, Qingdao, China*, in 2017. His research interests include man-machine system and non-destructive evaluation techniques.

Xiaokang Yin, received the B.E. degree in information engineering from *East China University of Science and Technology, Shanghai, China*, in June 2005. He continued with his postgraduate studies at the *University of Warwick, Coventry, U. K.*, from where he received the M.S. degree in advanced electronics engineering and Ph.D. degree in engineering, in January 2007 and May 2011, respectively. He, then, joins *China University of Petroleum, Qingdao, China* in November 2011, and is currently an Associate Professor at *Department of Mechanical and Electronics Engineering, China University of Petroleum, Qingdao, China*.

Chen Li, received the double B.E. degree both in mechanical design, manufacturing and automation and engineering management from *China University of Petroleum, Qingdao, China*, in 2016. He is currently working toward the M.E. degree in mechanical engineering with the research institute of *Center for Offshore Engineering and Safety Technology, China University of Petroleum, Qingdao, China*. His research interests include nondestructive testing especially in capacitive imaging, signal processing and inversion imaging.

Wei Li, received the Ph.D. degree in mechanical and electronics engineering from *China University of Petroleum, Qingdao, China*, in 2007. Following graduation, he joined *China University of Petroleum*, where he is currently a Professor of mechanical and electronics engineering. His current research interests include electromagnetic nondestructive evaluation and signal processing, offshore engineering structure design and FEM analysis, and pipeline safety and reliability assessment.

Guoming Chen, received the B.E. and M.E. degrees in petroleum mechanical engineering from *China University of Petroleum, Dongying, China*, in 1982 and 1986. He received the Ph.D. degree in mechanical design and theory from *China University of Petroleum*, in 1999. He is currently the Director of *Center for Offshore Engineering and Safety Technology, China University of Petroleum, Qingdao, China*. His research interests include offshore oil and gas equipment, troubleshooting and reliability assessment, and safety assessment. He has published more than 350 papers in the offshore oil and gas safety assessment field.

Funding

Supported by National Natural Science Foundation of China (Grant Nos. 51675536, 51574276), Fundamental Research Funds for the Central Universities of China (Grant No. 18CX02084A), and Innovative Talents Program of Far East NDT New Technology & Application Forum.

Competing Interests

The authors declare that they have no competing interests.

Received: 22 April 2019 Revised: 8 October 2019 Accepted: 19 November 2019

Published online: 05 December 2019

References

- [1] G Carra, V Carvelli. Long-term bending performance and service life prediction of pultruded Glass Fibre Reinforced Polymer composites. *Composite Structures*, 2015, 127: 308-315.
- [2] J Koyanagi, M Nakada, Y Miyano. Prediction of long-term durability of unidirectional CFRP. *Journal of Reinforced Plastics and Composites*, 2011, 30(15): 1305-1313.
- [3] J Tanks, S Sharp, D Harris, et al. Durability of CFRP cables exposed to simulated concrete environments. *Advanced Composite Materials*, 2017, 26(3): 245-258.
- [4] M A A Siddique, A A El Damatty. Enhancement of buckling capacity of steel plates strengthened with GFRP plates. *Thin-Walled Structures*, 2012, 60: 154-162.
- [5] C Meola, S Boccardi, G M Carlomagno, et al. Nondestructive evaluation of carbon fibre reinforced composites with infrared thermography and ultrasonics. *Composite Structures*, 2015, 134: 845-853.
- [6] J Dong, B Kim, A Locquet, et al. Nondestructive evaluation of forced delamination in glass fiber-reinforced composites by terahertz and ultrasonic waves. *Composites Part B: Engineering*, 2015, 79: 667-675.
- [7] X Zhang, X Wu, Y He, et al. CFRP barely visible impact damage inspection based on an ultrasound wave distortion indicator. *Composites Part B: Engineering*, 2019, 168: 152-158.
- [8] S C Garcea, Y Wang, P J Withers. X-ray computed tomography of polymer composites. *Composites Science and Technology*, 2018, 156: 305-319.
- [9] J F Florez-Ospina, H D Benitez-Restrepo. Toward automatic evaluation of defect detectability in infrared images of composites and honeycomb structures. *Infrared Physics & Technology*, 2015, 71: 99-112.
- [10] S Mukherjee, A Tamburrino, M Haq, et al. Far field microwave NDE of composite structures using time reversal mirror. *NDT & E International*, 2018, 93: 7-17.
- [11] K Mizukami, Y Mizutani, A Todoroki, et al. Detection of in-plane and out-of-plane fiber waviness in unidirectional carbon fiber reinforced composites using eddy current testing. *Composites Part B: Engineering*, 2016, 86: 84-94.
- [12] K Mizukami, Y Mizutani, K Kimura, et al. Detection of in-plane fiber waviness in cross-ply CFRP laminates using layer selectable eddy current method. *Composites Part A: Applied Science and Manufacturing*, 2016, 82: 108-118.
- [13] Y He, G Tian, M Pan, et al. Impact evaluation in carbon fiber reinforced plastic (CFRP) laminates using eddy current pulsed thermography. *Composite Structures*, 2014, 109: 1-7.
- [14] L Cheng, G Y Tian. Surface crack detection for carbon fiber reinforced plastic (CFRP) materials using pulsed eddy current thermography. *IEEE Sensors Journal*, 2011, 11(12): 3261-3268.
- [15] Y He, G Tian, M Pan, et al. Non-destructive testing of low-energy impact in CFRP laminates and interior defects in honeycomb sandwich using scanning pulsed eddy current. *Composites Part B: Engineering*, 2014, 59: 196-203.
- [16] F M Al-Oqla, S M Sapuan, T Anwer, et al. Natural fiber reinforced conductive polymer composites as functional materials: A review. *Synthetic Metals*, 2015, 206: 42-54.
- [17] H Sohn, D Dutta, J Y Yang, et al. Delamination detection in composites through guided wave field image processing. *Composites Science and Technology*, 2011, 71(9): 1250-1256.
- [18] C A C Leckey, M D Rogge, F Raymond Parker. Guided waves in anisotropic and quasi-isotropic aerospace composites: Three-dimensional simulation and experiment. *Ultrasonics*, 2014, 54(1): 385-394.
- [19] Z Wang, G Tian, M Meo, et al. Image processing based quantitative damage evaluation in composites with long pulse thermography. *NDT & E International*, 2018, 99: 93-104.
- [20] W Li, Y Xu, X Qing, et al. Quantitative imaging of surface cracks in polymer bonded explosives by surface wave tomographic approach. *Polymer Testing*, 2019, 74: 63-71.
- [21] X Yin, D A Hutchins, G Chen, et al. Studies of the factors influencing the imaging performance of the capacitive imaging technique. *NDT & E International*, 2013, 60: 1-10.
- [22] D Chen, X Hu, W Yang. Design of a security screening system with a capacitance sensor matrix operating in single-electrode mode. *Measurement Science and Technology*, 2011, 22(11): 114026.
- [23] Y Huang, Z Zhan, N Bowler. Optimization of the coplanar interdigital capacitive sensor. *AIP Conference Proceedings*, 2017, 1806(1).
- [24] X Yin, D A Hutchins, G Chen, et al. Detecting surface features on conducting specimens through an insulation layer using a capacitive imaging technique. *NDT & E International*, 2012, 52: 157-166.
- [25] S C Mukhopadhyay, C P Gooneratne. A novel planar-type biosensor for noninvasive meat inspection. *IEEE Sensors Journal*, 2007, 7(9): 1340-1346.
- [26] S Gholizadeh. A review of non-destructive testing methods of composite materials. *Procedia Structural Integrity*, 2016, 1: 50-57.
- [27] R T Sheldon, N Bowler. An interdigital capacitive sensor for nondestructive evaluation of wire insulation. *IEEE Sensors Journal*, 2014, 14(4): 961-970.
- [28] M Morozov, W Jackson, S G Pierce. Capacitive imaging of impact damage in composite material. *Composites Part B: Engineering*, 2017, 113: 65-71.
- [29] X Yin, D A Hutchins, G Chen, et al. Investigations into the measurement sensitivity distribution of coplanar capacitive imaging probes. *NDT & E International*, 2013, 58: 1-9.
- [30] S Laflamme, M Kollosche, J J Connor, et al. Soft capacitive sensor for structural health monitoring of large-scale systems. *Structural Control and Health Monitoring*, 2012, 19(1): 70-81.
- [31] X Yin, G Chen, W Li, et al. Negative measurement sensitivity values of planar capacitive imaging probes. *AIP Conference Proceedings*, 2014, 1581(1): 1500-1504.
- [32] C Li, G Xian, H Li. Water absorption and distribution in a pultruded unidirectional carbon/glass hybrid rod under hydraulic pressure and elevated temperatures. *Polymers*, 2018, 10(6): 627.

Submit your manuscript to a SpringerOpen® journal and benefit from:

- Convenient online submission
- Rigorous peer review
- Open access: articles freely available online
- High visibility within the field
- Retaining the copyright to your article

Submit your next manuscript at ► [springeropen.com](https://www.springeropen.com)
